

Concealing messages at the atomic-thin level by reaching the limit of writing

Chao Hou

Peking University

Qirong Yang

Peking University

Jianxin Guan

Peking University <https://orcid.org/0000-0002-8984-7384>

Jingwen Deng

Peking University

Zihan Xu

Shenzhen Six Carbon Tech Co. Ltd

Zhihao Yu

Peking University <https://orcid.org/0000-0002-6538-5007>

Junrong Zheng (✉ junrong@pku.edu.cn)

Peking University

Article

Keywords: Steganography, Single Molecular Layer Ink, P-type Doping, Photoluminescence, High-density Storage Media

Posted Date: December 8th, 2020

DOI: <https://doi.org/10.21203/rs.3.rs-111143/v1>

License:  This work is licensed under a Creative Commons Attribution 4.0 International License.

[Read Full License](#)

Version of Record: A version of this preprint was published at Advanced Materials Technologies on October 27th, 2021. See the published version at <https://doi.org/10.1002/admt.202101089>.

Abstract

The evolution of writing system reflects the development of civilization. Using single molecular layer “ink” to record invisible messages on an atomic-layered paper represents the ultimate thinness of classical writing system and steganography. A stable and convenient atomic-thin information steganography under ambient conditions is realized by using a monolayer of water as ink, an atomic layer of MoS₂ as paper, and a laser as pen. Physically adsorbed monolayered water molecules produce p-type doping to the substrate MoS₂ monolayer, leading to the enhancement of its photoluminescence (PL). Information is written on a monolayer of MoS₂ by using laser to remove surface water with designed patterns and is read out by PL imaging. The information is transparent to visible light and can retain for many days until erased by a humidification treatment. The method reaches the thinnest limit of writing and achieves repeatable data storage on an atomic layer under ambient conditions, providing a promising approach to steganography and towards high-density storage media at the atomic-thin level.

Main Text

From prehistoric symbolic murals carved on caves by stone, to the confidential information written on letter paper by invisible ink, the continuous improvement of writing system has witnessed human progresses. A special type of writing, steganography, which is usually taken as a top secret, is evolving with time. The formulas of secret ink used in the First World War were ordered to remain hidden from the public in 2002¹, even though these secret writing methods merely stay at the primary level of chromogenic reaction. At the turn of this century, it was reported that the steganographic technique could be advanced to the molecular level by concealing secret messages in DNA-based microdot^{2,3} and macromolecules⁴. By thinning down paper and ink to the atomic scale, one may reach the limit of writing system and take steganography a step further, even enabling the storage of data in an atomic-thin memory. The path to store information at the atomic limit can be carried out by scanning probe microscopes (SPM), e.g. scanning tunneling microscope (STM) through directly manipulating lattice locations^{5,6}, charge states^{7,8} or magnetization states⁹⁻¹¹, or atomic force microscope (AFM) methods like dip-pen nanolithography (DPN)¹²⁻¹⁴ that can deliver a wide range of substances onto various substrates^{13,15,16}. The SPM methods require low temperature, clean surface, ultrahigh vacuum environment and/or complicated operations^{17,18}, and their information readout typically relies on delicate SPM or electronic microscopes. These are undesirable features for steganography of which users are usually under intense pressure with limited conditions and have limited time to work.

Herein, using a monolayer of water as ink, an atomic layer of MoS₂ as paper, and a laser as pen, concealing information at the atomic-thin level is achieved under ambient conditions in a rewritable manner. The optical image of an n-doped MoS₂ monolayer is displayed in Fig. 1a. Its PL is enhanced upon water absorption, and the desorption of water by laser irradiation suppresses the PL enhancement, as shown in Fig. 1b. Raman spectroscopic measurements suggest that the laser irradiation does little damage to the MoS₂ monolayer. As displayed in Fig. 1c, absorbing H₂O molecules blueshifts and

intensifies the out-of-plane vibrational mode A_1' of MoS_2 , whereas the in-plane vibrational mode E' stays unchanged (blue line). After the laser irradiation treatment, the Raman spectrum (red line) changes back to be almost identical to the pristine one (black line), suggesting that there is little structural change within the monolayer of MoS_2 . To investigate the mechanism of PL enhancement by absorbing H_2O molecules, a field-effect transistor (FET) device is fabricated to explore the variations in carrier concentration of MoS_2 . Fig. 1d&e display the optical images of the FET device before and after adsorbing H_2O molecules, respectively. Their appearances look the same, but their electronic properties vary significantly. The source-drain current (I_{SD}) versus back gate voltage (V_{G}) curves in Fig. 1f indicate that the pristine device (black curve) shows an n-type characteristic. After absorbing H_2O molecules on the surface, the electron concentration drops sharply (blue curve), suggesting that the physically adsorbed H_2O molecules have a p-type doping to MoS_2 . A p-type doping favors the formation and recombination of neutral excitons over negative trions. According to literatures^{19–21}, neutral excitons have a faster radiative recombination rate than the negative trions and thus have a higher PL efficiency, leading to the PL enhancement. Once the absorbed H_2O molecules are erased by annealing in vacuum (200 °C for 3 h), the n-type characteristic (green curve) is restored, and in fact is even slightly enhanced compared to the pristine sample, because fewer water molecules are on the annealed sample.

The laser irradiation removing the surface H_2O molecules is further verified with AFM mapping. A square region by laser irradiation on the MoS_2 sample (the blue rectangle area denoted in Fig. 1a) is not distinguishable by optical microscope, whereas it is clearly visible under AFM mapping (Fig. 1g). The line profile in Fig. 1h indicates that the thickness of the monolayer MoS_2 before laser treatment is 1.43 nm, which is higher than the theoretical value of monolayered MoS_2 owing to the adsorbed water. The average thickness of the laser-treated square region (Fig. 1i) is measured to be 0.75 nm, consistent with the reported monolayer thickness of MoS_2 ²². The thickness reduction caused by laser treatment is about 0.68 nm, which agrees well with the thickness of a single layer of water molecules (~ 0.4 nm) plus the adsorption equilibrium distance (~ 0.2 nm)²³. The measured thickness of MoS_2 monolayer with adsorbed water is consistent with previous theoretical studies^{24,25}.

By removing surface water in designed patterns with lasers and the re-addition of water by humidification, rewritable data-encoding and readout through simple PL mapping can be achieved. The encoding scheme is illustrated in Fig. 2a. The sample is moisturized before laser writing, and then patterns are written directly onto the MoS_2 monolayer with a laser by removing the surface water. A home-built laser writing system is used to conduct the information-writing process (Supplementary Fig. 1). The laser-written information is read out by PL imaging, and is erased by exposing the sample to a humid environment. Fig. 2b displays a Chinese character “福” with the meaning of benevolence that is written onto the MoS_2 monolayer. The writing of “福” (Fig. 2c) and the erasing of it with water absorption (Fig. 2d) don't produce observable changes on the sample's optical images. Through PL mapping, the written pattern is clearly visible (Fig. 2e). Under ambient conditions (humidity < 30%), the written pattern can last for at least one week. The pattern is successfully erased after the sample is placed in a humid

environment (relative humidity ~85% for about 10 minutes) (Fig. 2f). The PL spectra of the sample before any treatments (black curve), after laser writing (red curve), and after pattern-erasing by adsorbing H₂O molecules (blue curve) are displayed in Fig. 2g. They are very similar to those in Fig. 1b, of which the PL intensity is dependent on the surface water content as discussed above. During writing, the laser power density is carefully controlled at about 3.0×10^5 w/cm² to ensure that the thermal energy generated by MoS₂ photo-absorption is sufficient for the removal of water but below the MoS₂ damage threshold. Overwriting with too much laser power can cause permanent damages to the MoS₂ monolayer and the written pattern cannot be erased by adsorbing H₂O molecules (Supplementary Fig. 2).

The MoS₂ monolayer is rewritable for many times. Fig. 3 displays the PL images of “☒” written in the solid-filled form (upper panels) and erased (bottom panels) at the 1st, 10th, 20th, 50th cycle. The upper panels are taken after each writing. “☒” is still visible after 50 writing/erasing cycles. The PL images in the bottom panels are taken after each humidification treatment, showing that “☒” is completely removed by the erasing process. To test how long the written pattern can last, we keep the sample in a container at 30% relative humidity (RH) for a week right after the 20th writing. Water in the air has not been able to erase the written pattern for such a long period of time, and “☒” is still clearly distinguishable, as shown in the upper 20th panel in Fig. 3. The corresponding optical images of the sample after each writing/erasing cycle also show no noticeable changes on the MoS₂ monolayer during the processes (Supplementary Fig. 3).

Not only can a simple word or symbol be written with the method, but also a sentence and even a painting. The phrase “Nothing is Impossible” (Fig. 4c) and the famous painting Mona Lisa (Fig. 4f) are successfully written on continuous MoS₂ monolayered films. The line drawing of Mona Lisa (Fig. 4f) is probably the thinnest portrait by far, since the “paper” is a monolayer of MoS₂ and the “pigment” is one layer of H₂O molecules.

The writing/erasing process is reasonably fast, dependent on the complexity of the written pattern. A more complexed pattern takes a longer time. With the same condition, writing “☒” and “π” of a similar size takes about 60 s and 15 s, respectively. It takes shorter than 10 mins to obtain their PL images by mapping. The erasing can be extremely fast. In a destructive way, if the sample is dipped into water or blown by breath, the pattern disappears immediately, but, in most of our tries the MoS₂ monolayer is broken after the erasing process. In a nondestructive manner, the sample is placed in an environment with a RH of 85%, the written pattern disappears within 10 minutes. In total, it takes minutes for the entire writing/erasing/readout process. The time can be significantly shortened by optimizing the operation conditions and tools, e.g. using 2D PL imaging rather than point mapping used in this work can cut the readout time from minutes to seconds, and using a pulsed laser that can deliver enough heat to desorb water molecules before the thermal energy diffuses out of the focus spot would increase both the writing speed and the spatial resolution.

In summary, atomic-thin erasable and rewritable information recorded on a MoS₂ monolayer under ambient conditions is achieved by modulating and imaging the PL of a MoS₂ monolayer with surface water reversible absorption/desorption. The messages encoded in this way can be at least under triple protections: information is encrypted, the writing appearance is invisible, and the designated MoS₂ triangle is camouflaged among a jumble of MoS₂ triangles; and they can be easily and immediately erased by breath or even saliva. The miniaturization of the equipment needed for the writing/readout processes is feasible and their operations can be foolproof. These are desirable and promising features for many applications, e.g. steganography, anti-counterfeiting, sensors, and transient information storage.

References

1. United States District Court for the District of Columbia, *The James Madison Project v. National Archives & Records Administration*, **CA98-2737**, 2002.3.5.
2. Clelland, C., Risca, V. & Bancroft, C. Hiding messages in DNA microdots. *Nature* **399**, 533–534 (1999)
3. Goldman, N. *et al.* Towards practical, high-capacity, low-maintenance information storage in synthesized DNA. *Nature* **494**, 77–80 (2013).
4. Cavallini, M. *et al.* Information Storage Using Supramolecular Surface Patterns. *Science* **299**, 531–531 (2003).
5. Bennewitz, R. *et al.* Atomic scale memory at a silicon surface. *Nanotechnology* **13**, 499–502 (2002).
6. Kalff, F. E. *et al.* A kilobyte rewritable atomic memory. *Nature Nanotechnology* **11**, 926–929 (2016).
7. Garcia, V. & Bibes, M. Ferroelectric tunnel junctions for information storage and processing. *Nature Communications* **5**, 1–12 (2014).
8. Repp, J., Meyer, G., Olsson, F. E. & Persson, M. Controlling the Charge State of Individual Gold Adatoms. *Science* **305**, 493–495 (2004).
9. Natterer, F. D. *et al.* Reading and writing single-atom magnets. *Nature* **543**, 226–228 (2017).
10. Loth, S., Baumann, S., Lutz, C. P., Eigler, D. M. & Heinrich, A. J. Bistability in Atomic-Scale Antiferromagnets. *Science* **335**, 196–199 (2012).
11. Kiraly, B. *et al.* An orbitally derived single-atom magnetic memory. *Nature Communications* **9**, 1–8 (2018).
12. Piner, R. D., Zhu, J., Xu, F., Hong, S. & Mirkin, C. A. ‘Dip-Pen’ Nanolithography. *Science* **283**, 661–663 (1999).
13. Ginger, D. S., Zhang, H. & Mirkin, C. A. The Evolution of Dip-Pen Nanolithography. *Angewandte Chemie International Edition* **43**, 30–45 (2004).
14. Salaita, K., Wang, Y. & Mirkin, C. A. Applications of dip-pen nanolithography. *Nature Nanotechnology* **2**, 145–155 (2007).
15. Ivanisevic, A. & Mirkin, C. A. “Dip-Pen” Nanolithography on Semiconductor Surfaces. *J. Am. Chem. Soc.* **123**, 7887–7889 (2001).

16. Liu, G., Hirtz, M., Fuchs, H. & Zheng, Z. Development of Dip-Pen Nanolithography (DPN) and Its Derivatives. *Small* **15**, 1900564 (2019).
17. Eigler, D. M. & Schweizer, E. K. Positioning single atoms with a scanning tunnelling microscope. *Nature* **344**, 524–526 (1990).
18. Stroscio, J. A. & Eigler, D. M. Atomic and Molecular Manipulation with the Scanning Tunneling Microscope. *Science* **254**, 1319–1326 (1991).
19. Mouri, S., Miyauchi, Y. & Matsuda, K. Tunable Photoluminescence of Monolayer MoS₂ via Chemical Doping. *Nano Lett.* **13**, 5944–5948 (2013).
20. Lien, D.-H. *et al.* Electrical suppression of all nonradiative recombination pathways in monolayer semiconductors. *Science* **364**, 468–471 (2019).
21. Nan, H. *et al.* Strong Photoluminescence Enhancement of MoS₂ through Defect Engineering and Oxygen Bonding. *ACS Nano* **8**, 5738–5745 (2014).
22. Tan, C. *et al.* Recent Advances in Ultrathin Two-Dimensional Nanomaterials. *Chem. Rev.* **117**, 6225–6331 (2017).
23. Yue, Q., Shao, Z., Chang, S. & Li, J. Adsorption of gas molecules on monolayer MoS₂ and effect of applied electric field. *Nanoscale Res Lett* **8**, 425 (2013).
24. Schumacher, A., Scandella, L., Kruse, N. & Prins, R. Single-layer MoS₂ on mica: studies by means of scanning force microscopy. *Surface Science* **289**, L595–L598 (1993).
25. Mieda, E. *et al.* Nanoprobe characterization of MoS₂ nanosheets fabricated by Li-intercalation. *Japanese Journal of Applied Physics* **54**, 08LB07 (2015).

Methods

Growth of monolayer MoS₂. Monolayer MoS₂ was grown on clean 285 nm thick SiO₂/Si wafers in a two-temperature-zone furnace via CVD method. MoO₃ powder (Alfa Aesar, 99.999%, 0.01 g) and sulfur powder (Alfa Aesar, 99.999%, 0.3 g) were used as solid sources. The crucible containing MoO₃ powder was placed 30 cm downstream of the sulfur boat. The SiO₂/Si substrate was positioned facing down at the location of 3 cm downstream from the MoO₃ boat. During growth, 300 sccm Ar gas was used as the carrier gas. After purging Ar gas for 20 min, the temperature for MoO₃ and sulfur powders was raised to 650 °C and 180 °C, respectively. Then the monolayer MoS₂ was obtained after ~7 mins of growth.

Laser writing and erasing. We used a home-built laser system to process the laser writing operation. The optical setup is illustrated in Supplementary Fig. 1, consisting of a microscopic system and a galvanometric scanning system. A continuous-wave solid-state laser diode (532 nm) was equipped as the laser writing source. We used a 60× objective lens to focus the laser spot into around 2.0 μm. The laser writing path according to the chosen pattern was designed by the software Autodesk (Autodesk Fusion 360). All laser writing processes were performed by using ~8 mW laser power at room temperature in ambient air. In particular, the laser spot should be accurately focused on the surface of the

monolayer MoS₂ to guarantee that the message can be effectively read and erased. The messages can be maintained at 30% RH at least one week. The erasing treatment was carried out by another humidification treatment.

PL/Raman and AFM measurements. In this work, we used a confocal Raman microscopic system (HORIBA, XploRA Plus) equipped with a 532 nm laser and a 100× objective lens to obtain PL mappings. The focused laser spot size on the sample was about 0.6 μm. 600 gr/mm gratings, 100 μm slit and 300 μm hole were adapted. The mapping step size is 0.3 μm with swift-on mode, and the integration time on each point is 0.04 s. All measurements were performed by using ~0.5 mW laser power at room temperature in ambient air. For the single point PL/Raman spectra, we used our home-built PL/Raman microspectroscopy with a 532 nm laser source and 50× long-working-distance objective lens (0.7 NA) which provides a spot size of ~2.5 μm. Typical excitation power was 5 mW, and the integration time was 10 s. We used 600 gr/mm grating and 300 μm slit to obtain PL spectra, and used 1800 gr/mm grating and 50 μm slit to acquire Raman spectra. Thickness variations of the samples were conducted with the tapping mode by using a commercial atomic force microscope (AFM, Bruker Dimension Icon with Nanoscope V controller).

Device fabrication and testing. To fabricate the FET device, polymethyl methacrylate (PMMA, Microchem, 495 K, A6) was firstly spin-coated onto the sample as the mask. We adapted Auto CAD to design an area in order to remove the undesired triangle domains within a 200 × 200 μm region around the target MoS₂ single domain. This designed area was then exposed by conducting high-resolution electron beam lithography (EBL). Through a precise oxygen plasma etching process, the exposed areas were etched, followed by a subsequent rinse with acetone to remove the top PMMA layer. Next, a second lithography was performed to create the source and drain electrode patterns. Cr/Au (5 nm / 45 nm) electrodes were thermally evaporated onto the substrate, and then acetone was used to remove the PMMA mask. Finally, the device was annealed in vacuum at 200 °C for 3 h to eliminate PMMA residuals and any moisture. The electrical characterizations of the MoS₂ FET device were carried out in ambient air on a probe station using a Keithley 4200 SCS as the parameter analyzer.

Data availability The data that support the findings of this study are available from the corresponding author on reasonable request.

Declarations

Acknowledgements The work is supported by the National Science Foundation of China (NSFC-21627805, 21673004, 21804004, and 21821004) and MOST (2017YFA0204702) China. The PL mappings were performed at HORIBA Scientific office (Beijing, China), and the electrical characteristics of FET devices were carried out at Prof. Jian Pei's lab in the college of Chemistry and Molecular Engineering

in Peking University. The authors thank the help offered by Dr. Yilin Lu, Dr. Teng Tu and Dr. Zefan Yao for the measurements of the mappings and electrical results.

Author contributions C.H. and J.Z. designed experiments. C.H. and Q.Y. conducted experiments. J.G. fabricated the FET devices. J.D. helped develop the PL/Raman microspectroscopy. Z.X. prepared the MoS₂ monolayers. Z.Y. designed and built the laser writing system. C.H. and Q.Y. analyzed data. C.H., Q.Y. and J.Z. prepared the manuscript. J.Z. supervised the project. All authors made critical contributions to the work.

Competing interests The authors declare no competing interests.

Additional information

Correspondence and requests for materials should be addressed to J.Z. (junrong@pku.edu.cn).

Figures

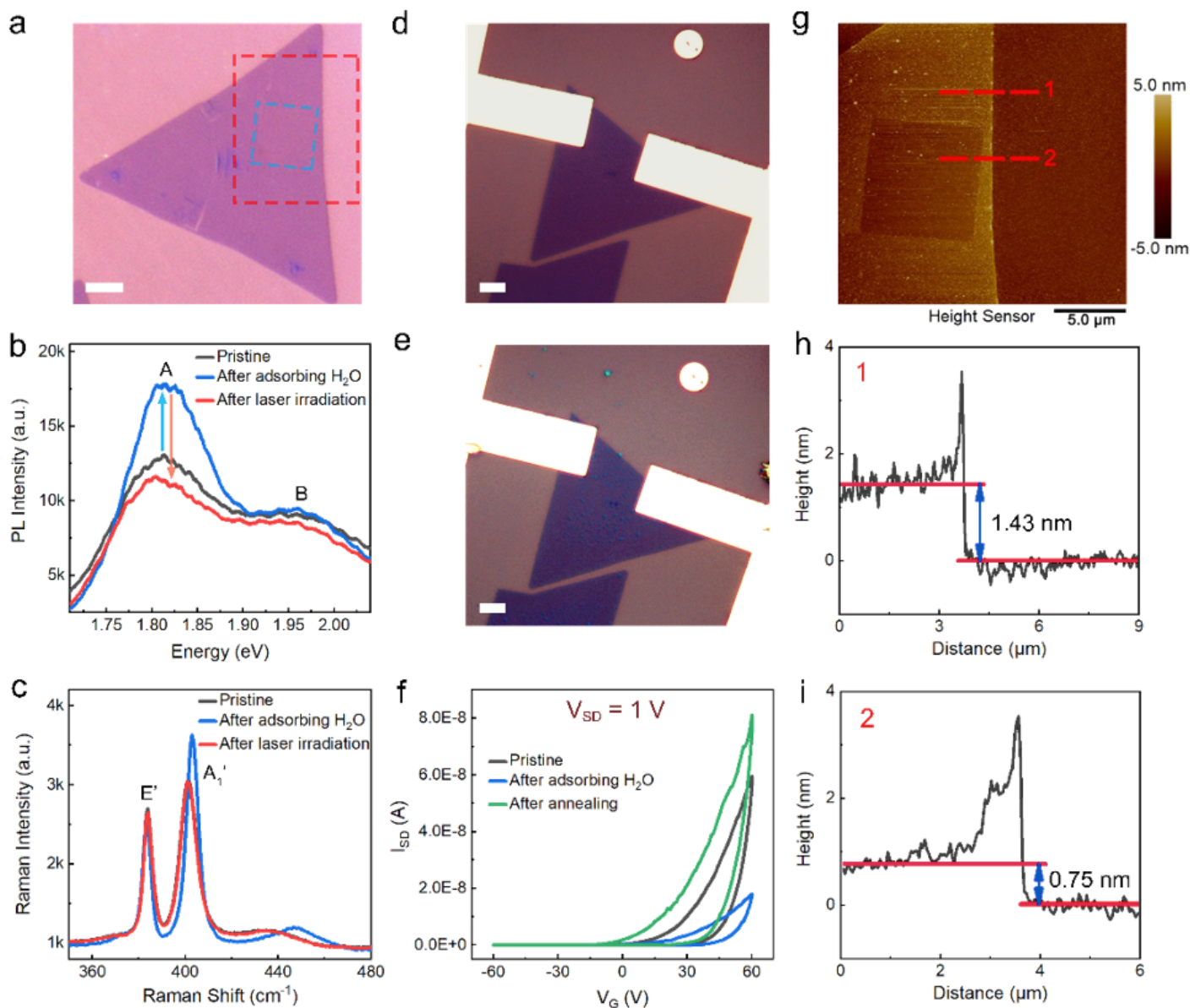


Figure 1

The PL enhancement and recovery of MoS₂ monolayer. a, Optical image of a monolayered MoS₂ triangle domain. b&c, The PL and Raman spectra of the MoS₂ monolayer before and after corresponding treatments. d&e, Optical images of the monolayered MoS₂ FET device before and after absorbing H₂O molecules. f, Source-drain current (I_{SD}) versus back gate voltage (V_G) curves with a source-drain voltage (V_{SD}) of 1 V for the FET device before and after corresponding treatments. g, AFM image for the red rectangle area in a, including the laser-treated region denoted with blue rectangle. h&i, A line profile showing the height along the red line #1 and #2 in g. Scale bars are all 5 μm .

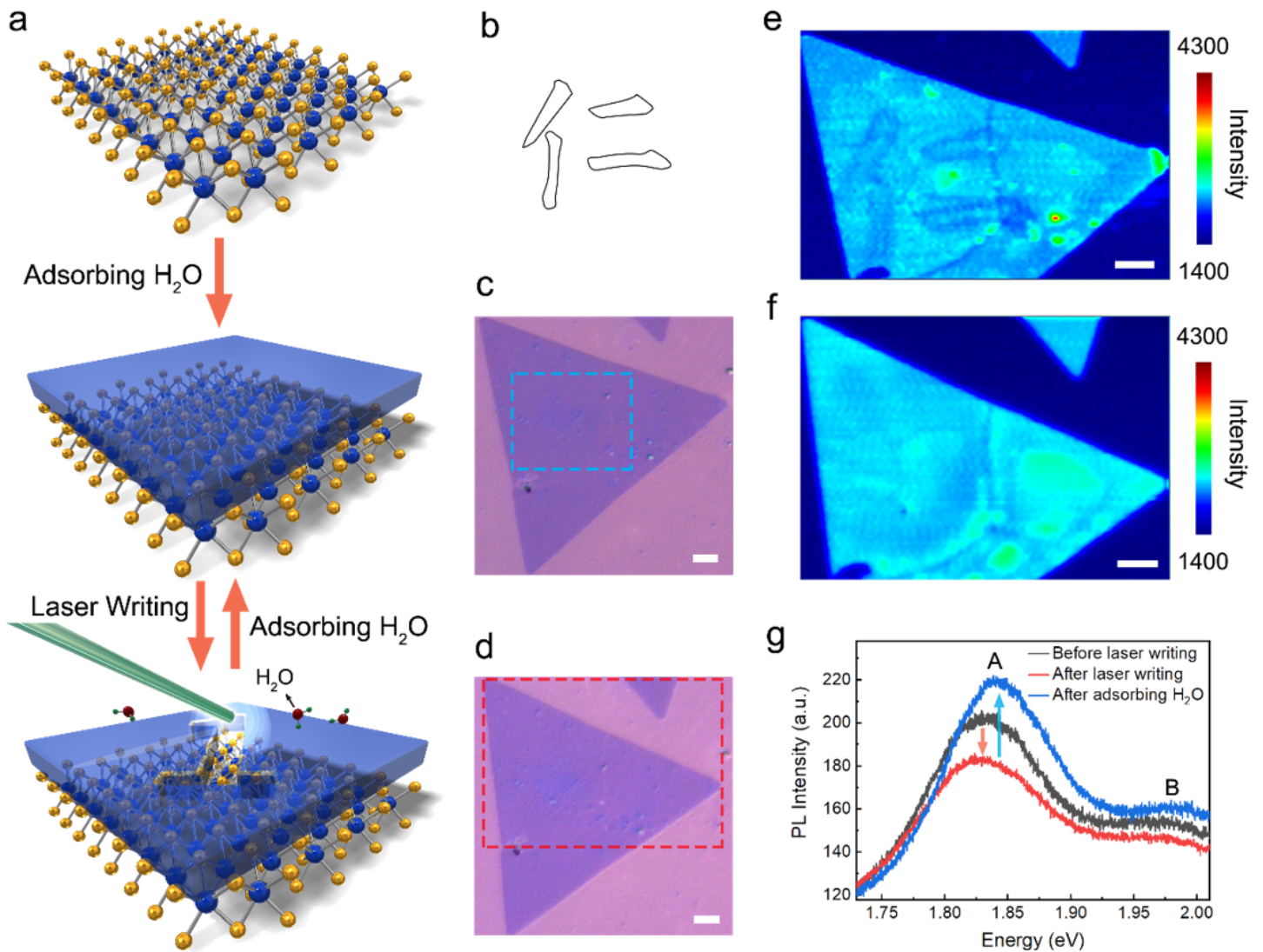


Figure 2

Laser writing and erasing on MoS₂ monolayer. a, A scheme of laser writing and erasing cycle. b, A Chinese character meaning “benevolence” used as a laser irradiation pattern. c, Optical image of a MoS₂ monolayer triangle domain after laser writing “仁” inside the blue rectangle. d, Optical image of c after erasing the pattern by adsorbing H₂O molecules. The red rectangle denotes the area being mapped. e&f, PL mapping images (at 1.82-2.00 eV) corresponding to c and d, respectively. g, PL spectra of the sample before (black curve) and after laser writing (red curve), and after erasing treatment (blue curve), respectively. Scale bars are all 4 μm.

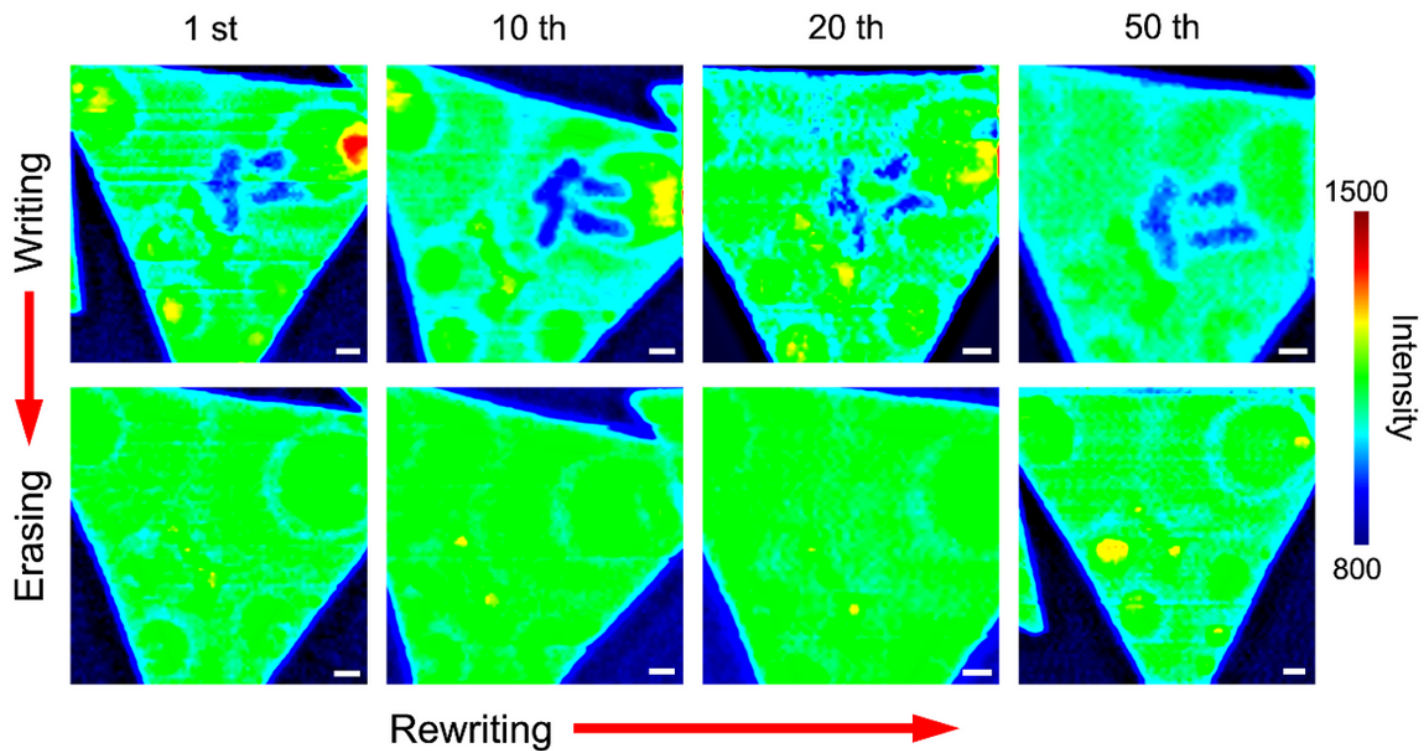


Figure 3

Repeatable laser writing and erasing on MoS₂ monolayer. The PL mapping for the 1st, 10th, 20th, 50th laser writing (upper panels) and erasing (bottom panels) “12” on the same MoS₂ monolayer triangle domain. Scale bars are all 2 μm.

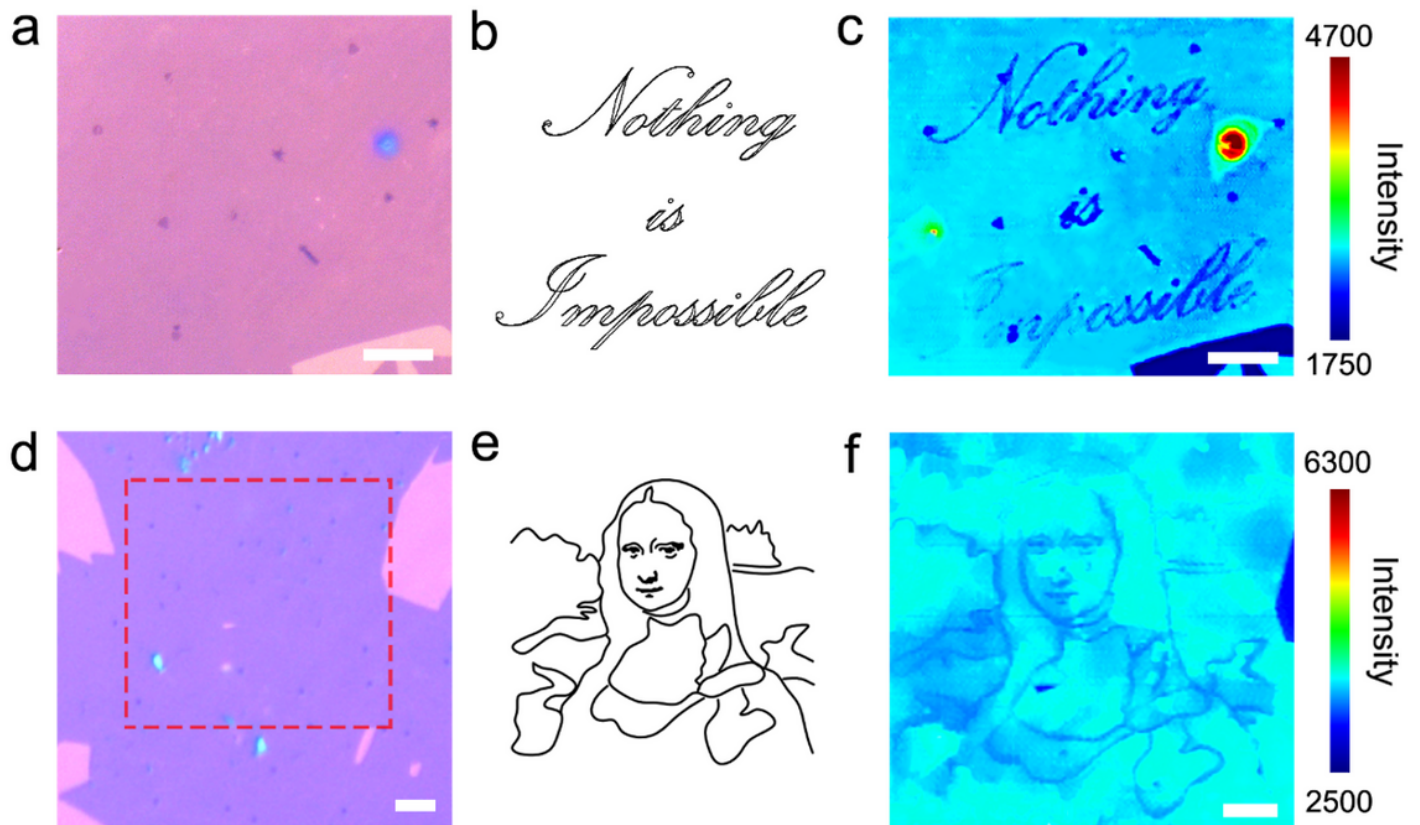


Figure 4

Complex patterns written on continuous film of MoS₂ monolayer. a, Optical image of one MoS₂ continuous film monolayer. b, A figure of the phrase “Nothing is Impossible” used as a pattern. c, The PL image corresponding to a that has been written with the phrase by laser. d, Optical image of another monolayered MoS₂ continuous film. The red rectangle denotes the area being mapped. e, A sketch of the famous painting Mona Lisa used as a pattern. f, The PL image corresponding to d showing the Mona Lisa painting created by laser writing. Scale bars are all 10 μm.

Supplementary Files

This is a list of supplementary files associated with this preprint. Click to download.

- [SI20201118.docx](#)